

## Exponential blocking-temperature distribution in ferritin extracted from magnetization measurements

T. H. Lee,<sup>1</sup> K.-Y. Choi,<sup>2</sup> G.-H. Kim,<sup>3</sup> B. J. Suh,<sup>4</sup> and Z. H. Jang<sup>1,\*</sup>

<sup>1</sup>*Department of Physics, Kookmin University, Seoul 136-702, Korea*

<sup>2</sup>*Department of Physics, Chung-Ang University, Seoul 156-756, Korea*

<sup>3</sup>*Department of Physics, Sejong University, Seoul 143-747, Korea*

<sup>4</sup>*Department of Physics, The Catholic University of Korea, Bucheon 420-743, Korea*

(Received 21 April 2014; revised manuscript received 21 July 2014; published 10 November 2014)

We developed a direct method to extract the zero-field zero-temperature anisotropy energy barrier distribution of magnetic particles in the form of a blocking-temperature distribution. The key idea is to modify measurement procedures slightly to make nonequilibrium magnetization calculations (including the time evolution of magnetization) easier. We applied this method to the biomagnetic molecule ferritin and successfully reproduced field-cool magnetization by using the extracted distribution. We find that the resulting distribution is more like an exponential type and that the distribution cannot be correlated simply to the widely known log-normal particle-size distribution. The method also allows us to determine the values of the zero-temperature coercivity and Bloch coefficient, which are in good agreement with those determined from other techniques.

DOI: [10.1103/PhysRevB.90.184411](https://doi.org/10.1103/PhysRevB.90.184411)

PACS number(s): 75.75.-c, 75.78.-n, 81.07.-b

### I. INTRODUCTION

A recent development of nanotechnology has enabled fabrication of a lot of different types of magnetic nanoparticles for the purpose of utilization in various fields [1] including magnetic storage [2], magnetic resonance imaging contrast agent [3], hyperthermal heating for cancer treatment [4], etc. As the fabrication or synthesis technique develops, adequate characterization of the nanoparticle system becomes of great importance. For magnetic particles like ferritin, the anisotropy barrier (or blocking temperature) and magnetic moment are two key parameters which determine their magnetic behavior. Thus, there have been many attempts to derive the blocking-temperature distribution from experiments [5]. But, most of them, especially those techniques based on temperature-dependent magnetization measurements, ignore the time evolution of magnetization (relaxation effect) in the analysis. Also, in many reports, the blocking temperature is assumed to have a log-normal distribution following the log-normal size distribution extracted from transmission electron microscopy (TEM) measurements [6–11]. The “size-blocking temperature” correlation has not been proved and its validity should be verified with independent extraction of the blocking-temperature distribution.

Ferritin is a biomagnetic molecule multi-existent in many kinds of biological systems and is important for the function of iron storage and iron toxicity reducer in living organisms [12–14]. In ferritin, 24 units of polypeptides are woven into a hollow sphere with an outer diameter of  $\sim 12$  nm and an inner diameter of  $\sim 8$  nm [15]. The hollow space is filled with a magnetic material vaguely known as ferrihydrite and which is generally accepted to have antiferromagnetic order. The truncated lattice at the surface (surface defects) or internal crystalline defects (body defects) induce a magnetic moment in the core [16,17]. Because of the regularity of the size of the

internal hollow space, the magnetic core of ferritin has a very narrow size distribution with a mean diameter of  $\sim 5$  nm [18].

### II. NONEQUILIBRIUM MAGNETIZATION CALCULATION

To extract the blocking-temperature distribution in ferritin, we should be equipped with the proper analytical tools. We start with three assumptions:

(1) *The particles with the same chemical composition can be categorized uniquely in terms of the zero-field, zero-temperature anisotropy barrier  $E_{B0}^0$ .* The anisotropy barrier is widely adopted for the description of magnetic behavior of magnetic particles. However, this quantity is not well defined physically since it varies with field and/or temperature. This motivates us to introduce a zero-field, zero-temperature (ZFZT) anisotropy barrier, independent of temperature and field, as a parameter for the unique categorization of the particles. In conjunction with the knowledge of  $E_{B0}^0$ , the field and temperature dependence of the anisotropy barrier completes our understanding of the experimental data which are usually taken under finite field and at finite temperature. Also,  $E_{B0}^0$  is directly related to the ZFZT blocking temperature  $T_{B0}^0$  as  $\tau_M = \tau_0 \exp(E_{B0}^0/k_B T_{B0}^0)$ . In this expression,  $\tau_0$  is the characteristic time of moment flipping,  $k_B$  is the Boltzmann constant, and  $\tau_M$  is the characteristic timescale of measurement. It is noted that, according to the relation, extracting the ZFZT blocking temperature is equivalent to extracting the ZFZT anisotropy barrier distribution.

(2) *Zero-field blocking temperature and magnetic moment of a particle are proportional to each other.* Usually, the magnetic moment and zero-field anisotropy barrier of superparamagnetic particles are known to be proportional to each other [19]. The zero-temperature coercive field  $H_{C0}$  is known to be related to the zero-field energy barrier  $E_{B0}$  ( $=KV$ ) and the magnetic moment  $\mu$  of the particle as [20–22]  $H_{C0} = 2\alpha E_{B0}/\mu$  ( $\alpha$  is a phenomenological constant and, for the random orientation of the anisotropy axis, it is set to be 0.48).  $H_{C0}$  does not depend on the temperature or the field

\*zeehoonj@kookmin.ac.kr

or the size of the particle but is characteristic of the magnetic material of the particle. Thus  $E_{B0}$  (and  $T_{B0}$ ) and  $\mu$  of the particle should be proportional to each other.

(3) *The particles are noninteracting.* The thick protein shell of ferritin hinders exchange interactions between the magnetic cores of ferritin and only the dipolar interaction is possible [17,23] (the minimum distance between the magnetic cores is 4 nm). Thus one can safely assume that the magnetic cores of ferritin are noninteracting in the temperature range of usual measurements.

One direct logical consequence of the above assumptions is that the magnetization of an ensemble of magnetic particles at temperature  $T$  and external field  $H$  is expressed by

$$M(T, H) = \int_0^\infty m(T_{B0}^0; T, H) f(T_{B0}^0) dT_{B0}^0, \quad (1)$$

where  $m(T_{B0}^0; T, H)$  is the magnetization of a single particle of which the ZFZT blocking temperature is  $T_{B0}^0$ .  $f(T_{B0}^0)$  is a distribution function of the ZFZT blocking temperature. It is noted that  $m(T_{B0}^0; T, H)$  depends not only on  $T$  and  $H$  but also on the previous thermomagnetic history of the ensemble. A detailed expression for the single-particle magnetization at the end of certain thermomagnetic processes should be  $m(T_{B0}^0; T_i, T_f, H_i, H_f, \Delta t)$  where  $T_i$  is the initial temperature of the particle at the beginning of the thermomagnetic process,  $T_f$  is the final temperature of the particle at the end of the thermomagnetic process,  $H_i$  is the initial field at the beginning of the thermomagnetic process,  $H_f$  is the final field at the end of the thermomagnetic process, and  $\Delta t$  is the time interval of the process. Since this expression is quite lengthy, hereafter it is simplified to  $m(T_{B0}^0; T, H)$  as introduced in Eq. (1), and a detailed thermomagnetic history is described when needed.

The evolution of  $m(T_{B0}^0; T, H)$  under the variation of the temperature and/or the field is described with the Bloch equation

$$\frac{dm(T_{B0}^0; T, H)}{dt} = \frac{m_{\text{eq}}(T_{B0}^0; T, H) - m(T_{B0}^0; T, H)}{\tau(T_{B0}^0; T, H)}, \quad (2)$$

where  $m_{\text{eq}}(T_{B0}^0; T, H)$  is the equilibrium magnetization of the particle at  $T$  and  $H$ , and  $\tau(T_{B0}^0; T, H)$  is the characteristic relaxation time of the particle at  $T$  and  $H$  and is given in terms of the Arrhenius law. The differential equation can be solved numerically for given experimental conditions—temperature, field, and thermomagnetic history. For better understanding of the characteristics of  $m(T_{B0}^0; T, H)$ , a new quantity is defined as  $R(T_{B0}^0; T, H) \equiv m(T_{B0}^0; T, H)/m_{\text{eq}}(T_{B0}^0; T, H)$ .  $R$  measures the degree of relaxation;  $R = 1$  for complete relaxation,  $0 < R < 1$  for incomplete relaxation, and  $R = 0$  for no relaxation. The distinction is very useful in nonequilibrium magnetization calculations. Equilibrium magnetization of a particle above the blocking temperature, in the superparamagnetic region, can be described with a Langevin function. Deviation of the measured magnetization from Langevin behavior in the blocked region is due to the blocking effect, which is *slow relaxation* rather than *complete freezing* of the moment. Thus, the equilibrium magnetization of a particle can be described with a Langevin function for all the temperature range below the critical temperature of the internal ordering if one is to measure “true” equilibrium magnetization with sufficiently

long measurement time;

$$m_{\text{eq}}(T_{B0}^0; T, H) = \mu(T) \left\{ \coth \left[ \frac{\mu(T)H}{k_B T} \right] - \left[ \frac{k_B T}{\mu(T)H} \right] \right\}, \quad (3)$$

where  $\mu(T)$  is envisaged as a spontaneous magnetic moment due to the internal ordering. The magnetic moment is proportional to  $K$  and  $E_{B0}$  as discussed before. Also, since  $H_{C0}$  is independent of temperature,  $\mu$  and  $K$  have the same temperature dependence,  $\mu(T)$ ,  $K(T) \propto (1 - BT^{3/2})$  [6,24,25]. Finally,  $\mu(T)$  can be written in terms of the ZFZT blocking temperature  $T_{B0}^0$  as

$$\mu(T) = \left( \frac{2\alpha k_B T_{B0}^0}{H_{C0}} \right) \ln \left( \frac{\tau_M}{\tau_0} \right) (1 - BT^{3/2}), \quad (4)$$

where  $B$  is the Bloch coefficient of the magnetic particle.

To solve Eq. (2) numerically, we also need a mathematical expression for the characteristic relaxation time  $\tau$  with explicit dependence on  $T_{B0}^0$  including the  $H$  dependence [8] as well as the  $T$  dependence, and the expression is

$$\tau = \tau_0 \left( \frac{\tau_M}{\tau_0} \right)^{\left[ \frac{T_{B0}^0}{T} (1 - BT^{3/2}) \left( 1 - \frac{H}{H_{C0}} \right)^{1.5} \right]}. \quad (5)$$

### III. ANALYSIS OF ZERO-FIELD-COOLED AND FIELD-COOLED MAGNETIZATION

Zero-field-cooled (ZFC) magnetization measurement consists of an initial field ramping-up step at the lowest temperature  $T_{\text{min}}$  and subsequent multiple temperature ramping-up steps (see Fig. 1).

Magnetization of the first data point can be described with the analytical expression  $R_1(T_{B0}^0) = 1 - \exp(-\tau_M/\tau)$ . As shown in Fig. 1(b), it is a blurred step function which can be approximated by a step function with a transition center at  $T_{B0,1}^{0,c}$ . Next, for the evolution of  $m(T_{B0}^0; T, H)$  in the subsequent temperature-ramping-up steps, we consider the process where the temperature changes from  $T_L$  to  $T_H$  with a constant-temperature sweeping rate and constant magnetic field. Let us assume that the magnetization of the ensemble of particles at  $T_L$  is described by  $R(T_{B0}^0; T_L, H)$ , which is the blurred step function of  $T_{B0}^0$ . Further evolution to temperature  $T_H$  can be calculated numerically with Eq. (2). The blurred step function is the generic feature of  $R(T_{B0}^0; T_H, H)$  which we verified with numerical calculations. The representative curves of  $R(T_{B0}^0; T_L, H)$  and  $R(T_{B0}^0; T_H, H)$  are shown in Fig. 1(b).

Combining all, the  $i$ th ZFC magnetization datum can be expressed as  $M_{\text{ZFC}}(T_i, H) \cong \int_0^{T_{B0,i}^{0,c}} m_{\text{eq}}(T_{B0}^0; T_i, H) f(T_{B0}^0) dT_{B0}^0$  with a step function approximation of  $R(T_{B0}^0; T_i, H)$ . The values of  $T_{B0,i}^{0,c}$  can be calculated numerically by integrating both functions,  $R(T_{B0}^0; T_i, H)$  and  $1 - \theta(T_{B0}^0 - T_{B0,i}^{0,c})$ . It is noted that the values of  $T_{B0,i}^{0,c}$  depend on  $H$ ,  $H_{C0}$ , and  $T_i$ , being quite different from  $T_i$ , the temperature of measurement.

Next, we approximate  $f(T_{B0}^0)$  as a piecewise linear function:  $f(T_{B0}^0) = \alpha_i T_{B0}^0 + \beta_i$ , in the range of  $T_{B0,i-1}^{0,c} < T_{B0}^0 < T_{B0,i}^{0,c}$  (where  $i = 1, 2, \dots$ ). With this approximation, we can

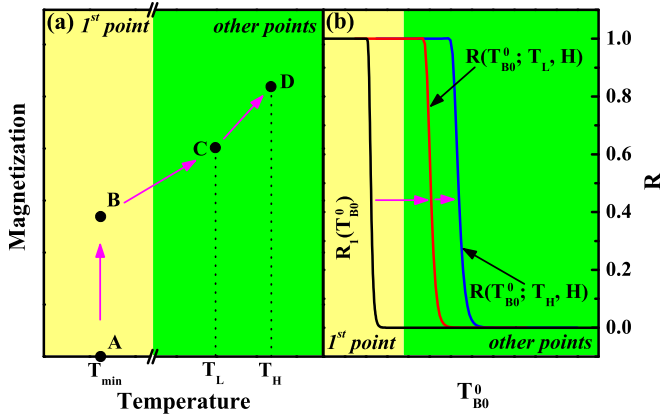


FIG. 1. (Color online) Magnetization evolution in ZFC process. (a) Magnetization evolution in  $M$ - $T$  space. (A to B) *First point*: Just after the field is turned on at  $T_{\min}$ , the magnetization of the particles is almost zero (point A). During the measurement, incomplete relaxation occurs due to the slow relaxation of some particles in the ensemble (point B). (C to D) *Other points*: For all subsequent data points, the magnetization evolves from a certain low temperature  $T_L$  (point C) to a certain high temperature  $T_H$  (point D). The evolution of magnetization in the steps depends on the temperature, the field, and the thermomagnetic history. (b) Description of magnetization evolution in terms of  $R(T_{B0}^0; T, H)$ . Representative curves of the functions,  $R_1(T_{B0}^0)$ ,  $R(T_{B0}^0; T_L, H)$ , and  $R(T_{B0}^0; T_H, H)$  are shown. The first data point is described in terms of  $R_1(T_{B0}^0)$ . One example of the subsequent evolution of magnetization is described as  $R(T_{B0}^0; T_L, H) \rightarrow R(T_{B0}^0; T_H, H)$ .

express the  $i$ th ZFC datum as

$$M_{\text{ZFC}}(T_i, H) \cong \sum_{n=1}^i \int_{T_{B0,n-1}^{0,c}}^{T_{B0,n}^{0,c}} (\alpha_n T_{B0}^0 + \beta_n) m_{\text{eq}}(T_{B0}^0; T_i, H) dT_{B0}^0, \quad (6)$$

where  $T_{B0,0}^{0,c}$  equals 0.

If there are  $N$  points in the ZFC magnetization data,  $f(T_{B0}^0)$  is approximated in  $N$  piecewise linear sections. Then, there are  $N$  equations of the form of Eq. (6),  $N-1$  continuity equations  $\alpha_i T_{B0,i}^{0,c} + \beta_i = \alpha_{i+1} T_{B0,i}^{0,c} + \beta_{i+1}$ , and one equation for the endpoint  $\alpha_N T_{B0,N}^{0,c} + \beta_N = 0$ . They constitute  $2N$  simultaneous linear equations. By solving these equations, the values of the  $2N$  variables,  $\alpha_i$ s and  $\beta_i$ s, i.e.,  $f(T_{B0}^0)$ , can be determined [26]. It is noted that the ZFZT blocking-temperature distribution is a function of  $H_{C0}$  and  $B$  even though it is extracted from ZFC data.

By reproducing field-cooled (FC) data with the extracted  $f(T_{B0}^0)$ , one can corroborate the validity of  $f(T_{B0}^0)$  and can also obtain the best values of  $H_{C0}$  and  $B$  at the same time. Similar to ZFC magnetization, FC magnetization, measured in the temperature-lowering process, is not an equilibrium quantity even though it is very close to that of equilibrium [24].

FC magnetization can also be calculated with Eqs. (1) and (2). The main difference is that the calculation is done without approximation since all  $R(T_{B0}^0; T, H)$  in the FC process do not show a blurred step-function behavior (see Fig. 2). In the ZFC process, small anisotropy-barrier particles relax completely to equilibrium at low temperature but big anisotropy-barrier

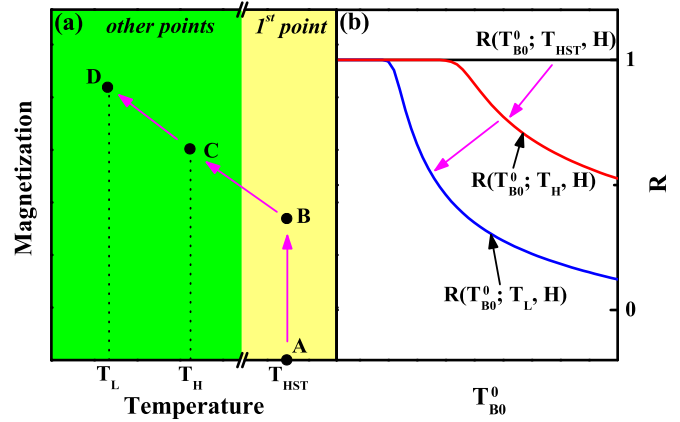


FIG. 2. (Color online) Magnetization evolution in FC process. (a) Magnetization evolution in  $M$ - $T$  space. (A to B) *First point*: At the highest temperature of our FC measurement ( $T_{\text{HST}}$ ), the maximum characteristic relaxation time of the particles is short compared with measurement time  $\tau_M$ . Thus, all particles are in the equilibrium state (point B). (C to D) *Other points*: For all the subsequent data points, magnetization evolves from a certain high temperature  $T_H$  (point C) to a certain low temperature  $T_L$  (point D). The evolution of magnetization in steps depends on the temperature, the field, and the thermomagnetic history. (b) Description of magnetization evolution in terms of  $R(T_{B0}^0; T, H)$ . Representative curves of the functions,  $R(T_{B0}^0; T_{\text{HST}}, H)$ ,  $R(T_{B0}^0; T_H, H)$ , and  $R(T_{B0}^0; T_L, H)$  are shown. Magnetization evolves as  $R(T_{B0}^0; T_{\text{HST}}, H) \rightarrow R(T_{B0}^0; T_H, H) \rightarrow R(T_{B0}^0; T_L, H)$  with decreasing temperature.

particles relax only at sufficiently high temperature. In the FC process, all particles start with nonzero magnetization at high temperature and some particles with a big anisotropy barrier swerve from equilibrium in the temperature-lowering steps.

To begin the calculation, one should know the initial magnetization of each particle at the highest temperature of the FC measurement. One can estimate the maximum characteristic relaxation time  $\tau_{\text{max}}$  of the particles at the highest temperature from the ZFZT blocking-temperature distribution with an Arrhenius law. If  $\tau_{\text{max}} \ll \tau_M$ , all particles are in the equilibrium state, as was the case for all of our results.

Thus, the calculated  $m(T_{B0}^0; T, H)$  is integrated with the piecewise linear form of  $f(T_{B0}^0)$  to obtain the FC magnetization;

$$M_{\text{FC}}(T, H) \cong \sum_{i=1}^N \int_{T_{B0,i-1}^{0,c}}^{T_{B0,i}^{0,c}} (\alpha_i T_{B0}^0 + \beta_i) m(T_{B0}^0; T, H) dT_{B0}^0. \quad (7)$$

#### IV. SAMPLE PREPARATION AND MAGNETIZATION MEASUREMENT

Natural horse spleen ferritin dissolved in a NaCl solution was purchased from Sigma Aldrich Chemicals, Inc. The ferritin sample was dialyzed extensively with distilled water to remove  $\text{Na}^+$  and  $\text{Cl}^-$  ions in the water. The dialyzed sample was then freeze dried to get samples in powder form for the experiments.

A conventional superconducting quantum interference device (SQUID) magnetometer (Quantum Design MPMS-7)

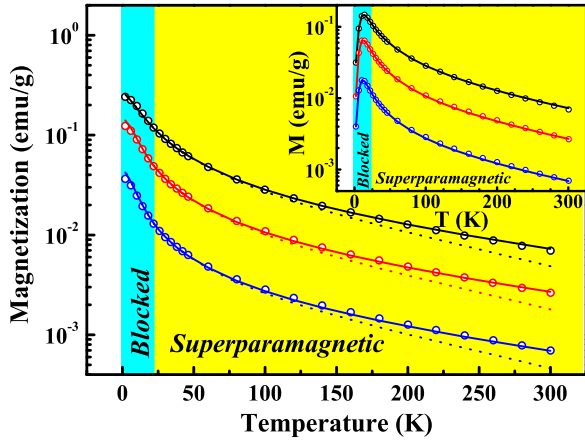


FIG. 3. (Color online) Fitting results of FC- and ZFC-magnetization data. Open circles are experimental data and solid lines are best-fit curves. Main panel shows FC magnetization and the inset shows ZFC one. The color of the symbols and lines designate the field strength: blue for  $H = 50$  Oe, red for  $H = 200$  Oe, black for  $H = 500$  Oe. For comparison, the fitting curves with  $B = 6.0 \times 10^{-5} \text{ K}^{-3/2}$  are shown as dotted lines. The distinction between “Blocked” and “Superparamagnetic” regions is made with  $T_{\max}$  [26].

was used to perform the ZFC and FC magnetization measurements on natural horse spleen ferritin samples from 2 to 300 K at three different fields (50, 200, 500 Oe). The temperature change between the measurements was set to be linear in time with negligible temperature-stabilization time. Non-negligible temperature stabilization time makes the nonequilibrium numerical calculation complex and hard. By using an internal function of the SQUID, the time elapsed between data points was also measured for the nonequilibrium-magnetization calculation. All data were corrected for the paramagnetic and/or diamagnetic background.

## V. EXTRACTED BLOCKING-TEMPERATURE DISTRIBUTION AND OTHER PARAMETERS

With a given set of  $H_{C0}$  and  $B$ , one can extract  $f(T_{B0}^0)$  from the ZFC data and calculate  $M_{\text{FC}}(T, H)$ . By changing the values of  $H_{C0}$  and  $B$ , we could perform the calculation iteratively to fit the FC-experiment data and could find the best values of  $H_{C0}$ ,  $B$  and extract the correct  $f(T_{B0}^0)$ . Beside  $H_{C0}$  and  $B$ , there are two other parameters which are related to the blocking behavior: the characteristic time of moment flipping  $\tau_0 = 1 \times 10^{-11} \text{ s}$  [6,21], and  $\tau_M \sim 10 \text{ s}$ , taken from a single SQUID measurement.

The fitting of the FC magnetization data for three different fields has been done with the corresponding ZFZT blocking-temperature distributions extracted from the ZFC data of the same fields. The results are shown in Fig. 3. As can be seen, the agreement between the fitting curves and experimental data is excellent. This demonstrates that our methodology successfully extracts the ZFZT blocking-temperature distribution and reproduces the measured FC magnetization curves.

We also obtained the best values of  $H_{C0} = 4130 \text{ Oe}$  and  $B = 3.0 \times 10^{-5} \text{ K}^{-3/2}$ . The measurements of the coercive

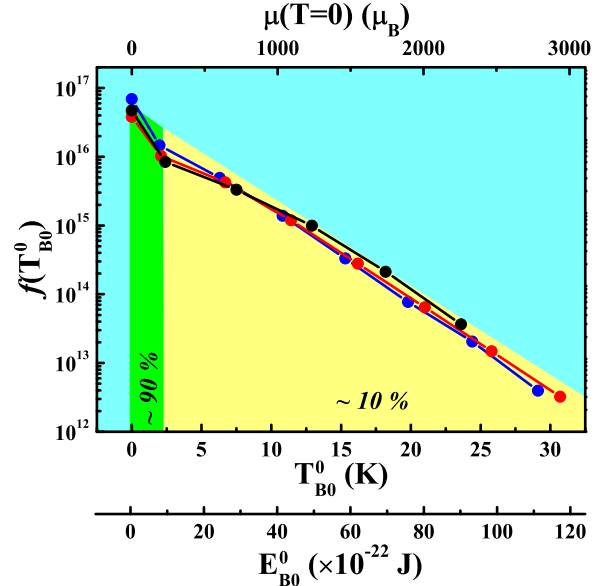


FIG. 4. (Color online) Extracted ZFZT anisotropy barrier, ZFZT blocking-temperature distribution, and zero-temperature magnetic-moment distribution. The ZFZT anisotropy barrier was calculated from  $T_{B0}^0$  with  $\tau_M = \tau_0 \exp(E_{B0}^0/k_B T_{B0}^0)$ . Also, the zero-temperature magnetic-moment distribution was calculated with Eq. (4) and the extracted  $f(T_{B0}^0)$ . The color of the lines designates field strength: blue for  $H = 50$  Oe, red for  $H = 200$  Oe, black for  $H = 500$  Oe. 90% of the magnetic particles have magnetic moment less than  $200\mu_B$  per particle (green region in the graph). Green and yellow regions designate exponential decay behavior of deduced ZFZT blocking-temperature distribution and zero-temperature magnetic-moment distribution. The extra abscissa for the ZFZT anisotropy energy barrier  $E_{B0}^0$  is shown underneath the abscissa of  $T_{B0}^0$ .

field of ferritin as a function of temperature had been reported before [27,28]. Extrapolation of the previously reported data to  $T = 0$  yielded  $H_{C0} \sim 4000 \text{ Oe}$  which is very close to our fitting result. By following the method described in Ref. [6],  $B$  was estimated to be  $6.0 \times 10^{-5} \text{ K}^{-3/2}$ . The value is of the same order of the magnitude as the result of FC magnetization fitting. As is evident from Fig. 3, our value better reproduces experimental data.

The ZFZT blocking-temperature distributions extracted from three different experiment data sets are shown in Fig. 4. The ZFZT blocking-temperature distribution should be independent of the magnetic field. Indeed, the extracted  $f(T_{B0}^0)$  graphs show that they are almost identical except for the termination of the data points at high field ( $H = 500 \text{ Oe}$ ). The explanation can be given as follows: what really affects experiment is a field- and temperature-dependent blocking-temperature distribution. At high field, the field-dependent blocking-temperature distribution is shrunk to lower region and the relatively high blocking-temperature region is not probed correctly.

## VI. DISCUSSION

With a log-normal size distribution of ferritin based on TEM observations and the assumption of uniformity of  $K$  with  $E_{B0} = KV$ , it is quite widely believed that the

anisotropy-barrier (or blocking-temperature) distribution is also of log-normal type. In contrast to the common belief, our analysis reveals an exponential-decay-type ZFZT blocking-temperature distribution. This strongly suggests that the anisotropy constant  $K$  is not sufficiently uniform to guarantee linearity between  $E_{B0}$  and  $V$ . Thus, the log-normal particle-size distribution cannot guarantee that the ZFZT blocking-temperature distribution is of log-normal type and there might not be a direct correlation between size distribution and blocking-temperature (or anisotropy-barrier) distribution.

By integrating the ZFZT blocking-temperature distributions for three different fields, we find that the number of particles with magnetic moment per gram ranges from  $5.8 \times 10^{16}$  to  $8.8 \times 10^{16}$ . With known molecular weight of horse spleen ferritin [29], a total number of ferritin particles per gram are calculated as  $\sim 9 \times 10^{17}$ . If we interpret this as it is, then it means the following: Most of the ferritin particles are magnetically inactive and only about 10% of the particles possess a magnetic moment. One may think the rest 90% of the particles possess magnetic moments, but they are inactive and blocked due to large anisotropy barrier at the temperatures of the measurements. But the close similarity between the maximum blocking temperature deduced directly from experimental data and that deduced from the extracted ZFZT blocking-temperature distribution excludes such a possibility unless there are particles with blocking temperatures higher than the maximum temperature of measurements (300 K). One may also think that 90% of the particles are paramagnetic rather than superparamagnetic with zero anisotropy barrier. But it is not in accordance with the fact that the reproduced FC magnetization with the extracted ZFZT blocking-temperature distribution is very close to the experiment data. Currently, we do not have a clear explanation of the finding but it should be checked and investigated in the future.

By using Eq. (4) and the extracted ZFZT blocking-temperature distribution, we calculated the distribution of the zero-temperature magnetic moment  $\mu(T=0)$ . The results are shown in Fig. 4 with the top abscissa as the independent parameter scale of  $\mu(T=0)$ . The zero-temperature magnetic-moment distribution shows that about 90% of the ferritin particles have a magnetic moment less than  $200\mu_B$ . Considering that most of the iron ions in the ferritin core are trivalent [30], we reach the conclusion that, for most of the magnetic ferritin particles, the magnetically active iron ion number does not exceed 50 per ferritin particle.

We have thus developed a method to extract the ZFZT blocking-temperature distribution in magnetic nanoparticle systems with a modified magnetization measurement procedure and a nonequilibrium magnetization calculation. We successfully applied the method to biomagnetic nanoparticle ferritin and extracted important magnetic parameters. The ZFZT blocking-temperature distribution in ferritin was found to be of exponential decay type, which is in stark contrast to the widely accepted log-normal distribution. We also found that almost 90% of ferritin particles are magnetically inactive. Our methodology is generic enough to be applied to the characterization of other magnetic nanoparticles.

## ACKNOWLEDGMENTS

This research was supported by the Basic Science Research Program through the National Research Foundation of Korea (NRF) funded by the Ministry of Education, Science and Technology (NRF-2008-314-C00123). We also acknowledge financial support from the Korea Research Foundation (KRF) grant funded by the Korea government (MEST) (Grant No. 2009-0076079). The work of G.H.K. was supported by the Basic Science Research Program through the National Research Foundation of Korea (NRF) funded by the Ministry of Education, Science and Technology (2011-0009747).

## APPENDIX

### 1. Characteristic relaxation time $\tau$

A mathematical expression of  $\tau$ , the characteristic relaxation time, is given in terms of an Arrhenius law as a function of  $T$  and  $H$  as

$$\tau = \tau_0 \exp \left[ \frac{E(H, T)}{k_B T} \right], \quad (\text{A1})$$

where  $\tau_0$  is the characteristic time for moment flipping,  $E(H, T)$  is the field- and temperature-dependent anisotropy barrier, and  $k_B$  is the Boltzmann constant. The blocking temperature  $T_B$  is usually defined to be the temperature at which the characteristic relaxation time is equal to the characteristic measurement timescale;  $\tau_M = \tau_0 \exp[E(H, T)/k_B T_B]$ . Since the anisotropy barrier is field and temperature dependent, it is better to define an invariant quantity ZFZT anisotropy barrier  $E_{B0}^0$  for the analysis. Thus, the ZFZT anisotropy barrier  $E_{B0}^0$  can be similarly related to the ZFZT blocking temperature  $T_{B0}^0$  as  $E_{B0}^0 = [k_B \ln(\tau_M/\tau_0)]T_{B0}^0$  where  $\tau_M$  is the characteristic timescale of measurement. Using the field dependence of the anisotropy energy barrier,  $[1 - (H/H_{C0})]^{1.5}$  (the exponent of 1.5 is used for random orientation of the anisotropy axis), and the temperature dependence of the anisotropy barrier,  $(1 - BT^{3/2})$ , the field- and temperature-dependent anisotropy barrier is given as a function of  $T_{B0}^0$  as

$$E(H, T) = \left[ k_B T_{B0}^0 \ln \left( \frac{\tau_M}{\tau_0} \right) \right] \times [1 - (H/H_{C0})]^{1.5} (1 - BT^{3/2}). \quad (\text{A2})$$

Now, substitute Eq. (A2) into the Arrhenius law to obtain the expression for the characteristic relaxation time  $\tau$  in terms of  $T_{B0}^0$ ,

$$\tau = \tau_0 \left( \frac{\tau_M}{\tau_0} \right)^{\left( \frac{T_{B0}^0}{T} \right) (1 - \frac{H}{H_{C0}})^{1.5} (1 - BT^{3/2})}. \quad (\text{A3})$$

### 2. Calculation of $R(T_{B0}^0; T_H, H)$

At  $T$ , the magnetization of an ensemble of particles can be expressed as

$$\begin{aligned} M_{\text{ZFC,FC}}(T, H) &= \int_0^\infty m(T_{B0}^0; T, H) f(T_{B0}^0) dT_{B0}^0 \\ &= \int_0^\infty R(T_{B0}^0; T, H) \\ &\quad \times m_{\text{eq}}(T_{B0}^0; T, H) f(T_{B0}^0) dT_{B0}^0. \end{aligned} \quad (\text{A4})$$

It is noted that  $m(T_{B_0}^0; T, H)$  can be a nonequilibrium quantity depending on the previous thermomagnetic history of the ensemble. The evolution of  $m(T_{B_0}^0; T, H)$  between the data points is described with the Bloch equation.

For the numerical calculation, the linear temperature increase between the data points was approximated with a multiple stepwise increase of the temperature. The effective temperature-sweeping rate was kept the same as that of the experimental linear increase of the temperature. The usual number of the steps in the numerical calculation was in the range of  $10 \sim 1000$ .

For each ‘‘microstep’’ of temperature, temperature was assumed to be constant and thus equilibrium magnetization is also invariant in the microstep ( $T$  is the temperature of the microstep). Then the solution of the Bloch equation for the microstep is

$$m_f(T_{B_0}^0; T, H) = m_{\text{eq}}(T_{B_0}^0; T, H) - [m_{\text{eq}}(T_{B_0}^0; T, H) - m_i(T_{B_0}^0; T, H)] \exp(-\Delta t/\tau), \quad (\text{A5})$$

where  $m_f(T_{B_0}^0; T, H)$  is the magnetization of the particle with ZFZT blocking temperature  $T_{B_0}^0$  at the end of the microstep and  $m_i(T_{B_0}^0; T, H)$  is the magnetization of the particle at the start of the microstep.  $\Delta t$  is the time interval of the microstep. For the particles with specific  $T_{B_0}^0$ , this calculation was performed successively up to the final temperature to get  $m$  and  $R$ . Also, the calculation can be performed for different  $T_{B_0}^0$  values to obtain  $R$  as a function of  $T_{B_0}^0$ .

Specifically in the ZFC magnetization calculations, the calculated results for  $R(T_{B_0}^0; T, H)$  showed blurred step-function behavior. The transition centers ( $T_{B_0}^{0,c}$ ) are related to the temperature of the measurement,  $T$ , but are not equal to  $T$ . The position of the transition center shifts toward higher  $T_{B_0}^0$  when  $T$  gets higher and/or when the time interval between the data points gets longer and/or when the field strength gets bigger. It is noted that, whatever are  $T$  or the time interval or field strength, the graphs of  $R(T_{B_0}^0; T, H)$  vs  $T_{B_0}^0/T_{B_0}^{0,c}$  are the same within the numerical calculation error.

### 3. Numerical calculation

We used a typical IBM PC with Windows XP operating system (32 bit). For a given set of values of  $B$  and  $H_{c0}$ , the calculation of FC data took a few minutes. The total calculation time for fitting with iteration depends on the initial values of the parameters and the fitting algorithm. We fit the data by manually changing the parameter values.

### 4. Magnetization relaxation

The relaxation of the magnetization of nanoparticles is known to have a  $\ln(t)$  time dependence and the magnetic viscosity  $S \equiv dM/d(\ln(t))$ , the slope of the relaxation curve, is known to be related to the blocking-temperature distribution [5,23,31]. Even though we are interested in the temperature-dependent magnetization measurements for extraction of the blocking-temperature distribution and the relaxation measurements have not been performed, it is also good to check whether our model reproduces the reported  $\ln(t)$  dependence

of magnetization relaxation in ferritin [31]. According to our model, time-dependent magnetization in the relaxation experiments can be expressed as

$$M(T, H, t) = \int_0^\infty m(T_{B_0}^0; T, H, t) f(T_{B_0}^0) dT_{B_0}^0, \quad (\text{A6})$$

where  $M(T, H, t)$  is the time-dependent magnetization of the nanoparticle system at  $T$ ,  $H$ , and time  $t$ ,  $m(T_{B_0}^0; T, H, t)$  is the time-dependent magnetization of a particle with ZFZT blocking temperature  $T_{B_0}^0$  at  $T$ ,  $H$ , and time  $t$ . With Eq. (A6) and the Bloch equation (2), we performed a nonequilibrium magnetization calculation numerically at the temperatures and time range reported in Ref. [31] and the results are shown in Fig. 5. Our calculation result is very similar to that of the previous report and the magnetization is indeed proportional to  $\ln(t)$ , at least in the time interval reported in Ref. [31]. The similarity between the experimental results and the nonequilibrium-calculation results implies that our model and methodology can explain the magnetization relaxation data as well. But a rigorous and quantitative check should be completed in the future by comparing with experiment.

Furthermore, we extended our nonequilibrium calculation of magnetization relaxation to a wider range of time and find that the magnetization relaxation is not completely linear with respect to  $\ln(t)$ , in contrast to the widely accepted linear dependence of magnetization with respect to  $\ln(t)$ . The nonlinear behavior becomes more evident at higher temperatures. This is not so surprising considering the fact that the relaxation eventually stops when the magnetization reaches zero and, at that point, the viscosity  $S$  should be zero. This fact also needs to be rigorously confirmed in future with separate experiments.

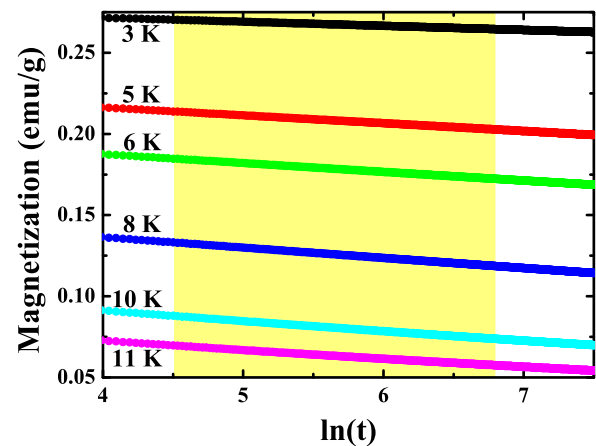


FIG. 5. (Color online) Time-dependent magnetization relaxation calculated with the extracted ZFZT blocking-temperature distribution from ferritin. At  $t = 0$ , the magnetic field was changed from 5 T to 0. The magnetization relaxation curves at  $T = 3, 5, 6, 8, 10,$  and  $11$  K are shown. The time range,  $4.5 < \ln(t) < 6.8$ , is highlighted for comparison with Fig. 1 in Ref. [31].

- [1] G. Reiss and A. Hütten, *Nat. Mater.* **4**, 725 (2005).
- [2] B. D. Terris and T. Thomson, *J. Phys. D: Appl. Phys.* **38**, R199 (2005).
- [3] H. B. Na, I. C. Song, and T. Hyeon, *Adv. Mater.* **21**, 2133 (2009).
- [4] C. D. Kaddi, J. H. Phan, and M. D. Wang, *Nanomedicine (London, UK)* **8**, 1323 (2013).
- [5] R. Zheng, H. Gu, B. Zhang, H. Liu, X. Zhang, and S. P. Ringer, *J. Magn. Magn. Mater.* **321**, L21 (2009).
- [6] F. Wiekhorst, E. Shevchenko, H. Weller, and J. Kötzler, *Phys. Rev. B* **67**, 224416 (2003).
- [7] E. F. Ferrari, F. C. S. da Silva, and M. Knobel, *Phys. Rev. B* **56**, 6086 (1997).
- [8] R. Sappey, E. Vincent, N. Hadacek, F. Chaput, J. P. Boilot, and D. Zins, *Phys. Rev. B* **56**, 14551 (1997).
- [9] F. Ludwig, E. Heim, and M. Schilling, *J. Appl. Phys.* **101**, 113909 (2007).
- [10] N. J. O. Silva, V. S. Amaral, and L. D. Carlos, *Phys. Rev. B* **71**, 184408 (2005).
- [11] S. Rohart, C. Raufast, L. Favre, E. Bernstein, E. Bonet, and V. Dupuis, *Phys. Rev. B* **74**, 104408 (2006).
- [12] A. Marchetti, M. S. Parker, L. P. Moccia, E. O. Lin, A. L. Arrieta, F. Ribalet, M. E. P. Murphy, M. T. Maldonado, and E. Virginia Armbrust, *Nature (London)* **457**, 467 (2009).
- [13] P. M. Harrison and P. Arosio, *Biochim. Biophys. Acta, Bioenerg.* **1275**, 161 (1996).
- [14] B. D. Schneider and E. A. Leibold, *Curr. Opin. Clin. Nutr. Metab. Care* **3**, 267 (2000).
- [15] D. M. Lawson, P. J. Artymiuk, S. J. Yewdall, J. M. A. Smith, J. Craig Livingstone, A. Treffry, A. Luzzago, S. Levi, P. Arosio, G. Cesareni, C. D. Thomas, W. V. Shaw, and P. M. Harrison, *Nature (London)* **349**, 541 (1991).
- [16] F. Brem, G. Stamm, and A. M. Hirt, *J. Appl. Phys.* **99**, 123906 (2006).
- [17] S. A. Makhlof, F. T. Parker, and A. E. Berkowitz, *Phys. Rev. B* **55**, R14717 (1997).
- [18] S. Mann, *Inorganic Materials* (Wiley, Chichester, 1996).
- [19] N. J. O. Silva, V. S. Amaral, L. D. Carlos, B. Rodríguez-González, L. M. Liz-Marzán, T. S. Berquó, S. K. Banerjee, V. de Zea Bermudez, A. Millán, and F. Palacio, *Phys. Rev. B* **77**, 134426 (2008).
- [20] E. C. Stoner and E. P. Wohlfarth, *Philos. Trans. R. Soc., A* **240**, 599 (1948).
- [21] R. K. Zheng, H. Gu, B. Xu, and X. X. Zhang, *J. Phys.: Condens. Matter* **18**, 5905 (2006).
- [22] E. Lima, A. L. Brandl, A. D. Arelaro, and G. F. Goya, *J. Appl. Phys.* **99**, 083908 (2006).
- [23] N. T. Gorham, T. G. St. Pierre, W. Chua-Anusorn, and G. M. Parkinson, *J. Appl. Phys.* **103**, 054302 (2008).
- [24] N. A. Usov, *J. Appl. Phys.* **109**, 023913 (2011).
- [25] B. D. Cullity and C. D. Graham, *Introduction to Magnetic Materials* (IEEE Press, John Wiley & Sons, Hoboken, 2009).
- [26] One can continue the calculation for all the  $T_i$ s in ZFC data but it is better to limit the calculation up to  $T_{\max}$  where ZFC magnetization data and FC magnetization data bifurcate because there is no blocking behavior above  $T_{\max}$ .
- [27] G. C. Papaefthymiou, *Biochim. Biophys. Acta, Gen. Subj.* **1800**, 886 (2010).
- [28] S. H. Kilcoyne and R. Cywinski, *J. Magn. Magn. Mater.* **140-144**, 1466 (1995).
- [29] C. F. A. Bryce and R. R. Crichton, *J. Biol. Chem.* **246**, 4198 (1971).
- [30] E. Lee, D. H. Kim, J. Hwang, K. Lee, S.-W. Yoon, B. J. Suh, K. H. Kim, J.-Y. Kim, Z. H. Jang, B. Kim, B. I. Min, and J.-S. Kang, *Appl. Phys. Lett.* **102**, 133703 (2013).
- [31] T. G. St. Pierre, N. T. Gorham, P. D. Allen, J. L. Costa-Krämer, and K. V. Rao, *Phys. Rev. B* **65**, 024436 (2001).